Sidahmed Ameur[1], Chikh Ould El Bahri[2], Abdelkader Djebli[2], Mostefa Bendouba[2], Abdelkrim Aid[2], Benattou Bouchouicha[1]*

ANALYSIS OF FSW PARAMETERS: NUMERICAL SIMULATION OF HDPE PLATE

ANALIZA ZTM PARAMETARA: NUMERIČKA SIMULACIJA HDPE PLOČE

Originalni naučni rad / Original scientific paper
UDK /UDC:

Rad primljen / Paper received: 21.04.2021

Adresa autora / Author's address:
[1)] University Djillali Liabess of Sidi Bel Abbess, Algeria
[2)] University Mostapha Stambouli of Mascara, Algeria
email: djebliabdelkader@yahoo.fr

Keywords
- friction stir welding (FSW)
- polyethylene
- thermomechanical
- FEM modelling
- heat transfer

Ključne reči
- zavarivanje trenjem sa mešanjem (ZTM)
- polietilen
- termomehanički
- modeliranje MKE
- prenos toplote

Abstract

A three dimensional coupled thermomechanical finite element model (FEM) is proposed. The aim is to simulate the friction stir welding (FSW) process of high density polyethylene (HDPE) materials. An optimisation study using a full factorial design has made it possible to distinguish the effects of welding parameters. The parameters taken into account are taken on two levels, the tool rotational speed, shoulder diameter, and pressure exerted by the tool. The temperature values generated by different combinations of parameters are analysed and the combination of optimal parameters is determined. Results show the dependence of maximum temperature on rotational speed. The generated temperature at the joint essentially determines the weld quality and tensile strength. Thus, a target temperature below the melting point of HDPE can be achieved through careful choice of FSW welding parameters.

Izvod

Predložen je spregnut termomehanički model konačnih elemenata (MKE). Cilj je da se simulira postupak zavarivanja trenjem sa mešanjem (ZTM) za slučaj polietilenskih materijala velike gustine (HDPE). Studija optimizacije preko potpunog faktorskog dizajna je omogućila da se izdvoje uticaji pojedinačnih parametara zavarivanja. Parametri koji su ovde uzeti u obzir su dva reda veličine: rotaciona brzina, prečnik i pritisak koji ostvaruje alat. Temperature generisane preko različitih kombinacija parametara su analizirane i određena je njihova optimalna kombinacija. Rezultati su pokazali da postoji zavisnost između maksimalne temperature i brzine rotacije. Temperatura generisana u zavarenom spoju suštinski određuje kvalitet zavara i njegovu zateznu čvrstoću. Stoga, ciljna temperatura ispod tačke topljenja HDPE materijala se može postići pravilnim izborom parametara zavarivanja za ZTM postupak.

INTRODUCTION

Friction stir welding (FSW) is a solid state welding process that uses a special tool to join two adjacent parts together without melting the material. It was invented by The Welding Institute (TWI) in 1991, /1/. Originally, the process is performed on aluminium alloys, but since then FSW has been used to join a large number of similar and dissimilar materials, /2-7/. Practically, the basic principle of the FSW process is the plunge of a special tool between two plates, then stir, deform, and mix the matter between the plate edges. So, heat is generated by friction between the rotary tool and plates, which plasticizes the material in the weld area /8-15/. The advantage over conventional welding processes is that FSW does not require any filler material, shielding gas, or other consumables, and consumes much less energy. It generates no harmful gases or welding burrs and produces little noise. The process actively contributes to improving working conditions, and at the same time increases productivity. Thanks to these unique advantages, new applications can be developed through FSW. It is now possible to weld materials that were previously impossible, such as high strength aluminium alloys, as well as the joining of polymer materials. Indeed, the last decade has marked much research that have been made to study the welding ability of thermoplastic materials using the FSW process /16-17/. Undoubtedly, polymers are now present in all industrial fields, such as transport, environment, energy, medical engineering. This explains the growing interest in these materials and therefore, the key step in the fabrication of polymer structures is closely dependent on the success of the assembly processes. Rightly so, due to the limitations of different joining techniques for polymers such as mechanical fastening, adhesive bonding, laser welding, including over-melting, scratching, vaporization, incomplete bonding and forming of cracks around the joint area, the FSW technique stands out as an alternative with prominent potential, /18/. Thus, researchers are increasingly focusing on the development of the FSW process for its integration into the industrial process involving the assembly of polymer structures, /19-21/. In this context, several studies axe on the effect of welding parameters on the quality and strength of the joint welded by FSW. However, the quality and strength of the welded joint are the direct result of thermal phenomena generated by friction between the tool and plates, as well as by plastic deformations during the mixing of the material under the shoulder and in contact with the pin, /22/. Therefore, many experimental studies have been carried out to optimise the welding parameters leading to better properties of joints /23-32/.

ANALYTICAL MODEL OF HEAT FLOW AROUND THE SHOULDER

The main object of this paper is to numerically analyse the effect of friction stir welding parameters on HDPE plates. A 3-D FE model is carried out beforehand by introducing, under a theoretical basis, the concepts of thermal phenomena produced during FSW welding. A focus was done on the effect of welding parameters considered to be the main important following literature documentation. These parameters are the pressure exerted by tool, the tool rotational speed, and its geometry reflected here, by the diameter of the shoulder. Thus, temperature measurements are taken as a result to be optimised for a successful welded joint. The temperature peaks in the welded zone are evaluated and analysed.

Concerning the heat transfer in FSW, it is assumed that heat generation by the pin has little or no effect on the temperature fields. The heat production of the shoulder will be considered as the only heat source in our model as assumed by /22/.

The relationship between contact pressure and contact shear stress can be prescribed by different friction models. In this work, it is assumed that the contact shear stress τ is described by Coulomb's law, expressed by the relation:

$$\tau_{\text{contact}} = \tau_{\text{friction}} = \mu P \,, \tag{1}$$

where: μ is the friction coefficient; and P is contact pressure.

Based on the hypothesis of heat generation, mainly through contact between the shoulder and the surface of the material, local heat generation at a surface segment on the tool/plate interface can be given by:

$$q = \tau_{\text{contact}} w_r \,, \tag{2}$$

where: τ_{contact} is shear stress located at the contact interface between the rotary tool and shear layer; and w_r is the rotational speed of the tool as a function of the position on the radius of the shoulder. By integrating Eq.(2) on the contact zone of the shoulder, the contribution of heat generation of the shoulder is estimated as:

$$Q_{\text{tool}} = \int_{R_{\text{pin}}}^{R_{\text{shoulder}}} \int_{0}^{2\pi} \tau_{\text{contact}} w r r d r d\theta = \int_{R_{\text{pin}}}^{R_{\text{shoulder}}} 2\pi w \tau_{\text{contact}} r^2 dr =$$

$$= \frac{2}{3}\pi w \tau_{\text{contact}} (R_{\text{shoulder}}^3 - R_{\text{pin}}^3) \,. \tag{3}$$

To get an idea of how much heat to expect in friction stir welding, Table 1 shows the heat generation contributions of a typical tool having a shoulder radius of 9 mm, a pin radius of 3 mm, and a pin height of 3 mm. A total heat generation of 1.4 kW is estimated for typical 3 mm thick aluminium alloy plates, where yield strength of 20 MPa is assumed to be descriptive of the material's resistance to elevated temperatures, /22/.

Table 1. Contribution of tool parts to the heat generation /22/.

Source	heat generated (W)	Relative contribution (%)
Q_{shoulder}	1230	87
$Q_{\text{pin lateral}}$	142	10
$Q_{\text{pin point}}$	47	3
Q_{tool}	1419	100

Thus, assuming a zero pin radius and substituting Eq.(1) in Eq.(3), we get:

$$Q = \frac{2}{3}\pi w R_{\text{shoulder}}^3 \mu P \,. \tag{4}$$

Estimating the pressure by:

$$P = \frac{F_Z}{A_{\text{tool}}} \,, \tag{5}$$

where: F_Z is the axial force of the tool; and A_{tool} is section of tool in contact with the plates to be welded, given by:

$$A_{\text{tool}} = \pi R_{\text{shoulder}}^2 \,. \tag{6}$$

Finally, the amount of heat generated by the shoulder is given by:

$$Q = \frac{2}{3} w R_{\text{shoulder}} \mu F_Z \,. \tag{7}$$

The friction coefficient μ varies between 0 and 0.6, where values of around 0.3 are often reported in literature, however, exact values for different welding conditions and tool/part combinations are difficult to measure.

NUMERICAL MODEL

Materials used in this work are steel for the tool (Fig. 1a) and high density polyethylene for the plates (Fig. 1b). The mechanical and thermal properties of these two materials are listed in Table 2.

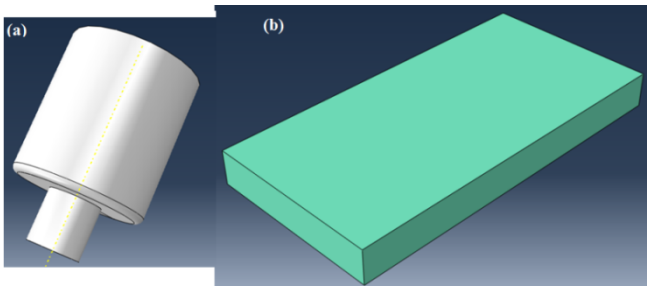

Figure 1. Model of the tool and HDPE plate.

Table 2. Physical and mechanical properties of materials in the study (HDPE and steel).

Characteristic	HDPE	Steel
density (kg/m^3)	950	7800
Young's modulus (Pa)	1.2×10^9	209×10^9
Poisson's coefficient	0.4	0.3
thermal conductivity (W/m K)	0.5	48
specific heat (J/K kg)	1900	452

The parameters of the FSW process analysed are for the speed of rotation of the tool, the forging force or pressure on the tool, and the diameter of the shoulder. These parameters are taken in two levels each, in order to then be able to plan the simulations and identify the effects and thus optimise the process. Table 3 summarizes the levels of these parameters.

Table 3. FSW parameters and their levels for joining HDPE sheets.

Parameters	Unit	Level	
		max	min
rotational speed	rpm	2000	500
shoulder radius	mm	10	5
pressure force	MPa	10	5

Modelling by finite element method is carried out using Abaqus® calculation code. Figure 2 shows the assembled model, and Fig. 3 shows the mesh for the plate and the tool. Mesh is performed with 8 tri-linear node brick element type. In addition, a thermal analysis requires displacement-thermal coupling elements of the C3D8T family.

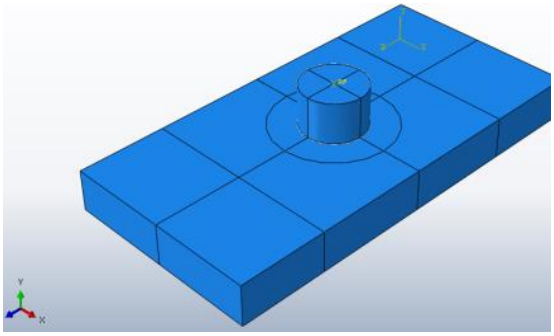

Figure 2. The model of the assembled plates.

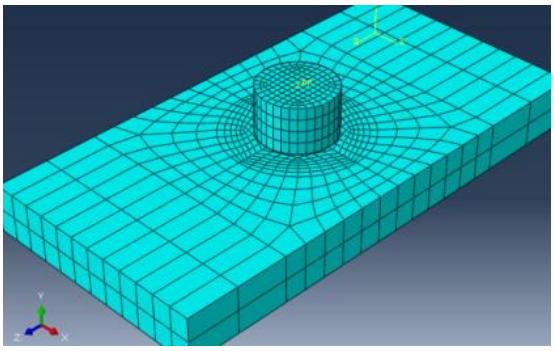

Figure 3. 3D mesh by C3D8T FE type.

To simulate the FSW welding process, we used boundary conditions that interpret reality as much as possible such as the machine table, the tool rotation, and its displacement along the machine axis. The initial temperature conditions are also imposed on the plate/tool assembly. In fact, Fig. 4a shows the boundary condition imposed on the lower surface of the plate, thus interpreting the fixing of the plate by a clamping system. Figure 4b shows the condition imposed on the tool by blocking movements along the *x* and *z* axes and blocking rotations around *x* and *z* axes. The tool has been attached to a reference point, where these conditions are imposed as well as the condition of rotation and pressure on the plate.

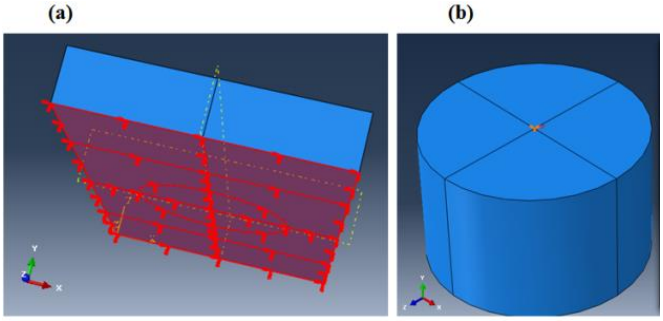

Figure 4. Boundary condition imposed to plates and tool.

Initial temperature conditions are imposed such that the temperature of the assembly is ambient, 20 °C.

Analysis type and contact definition

The current study relates with heat production, which represents the main phenomenon during welding operation. This is achieved by explicit coupling temperature-displacement. For the definition of the contact, it is used the surface/surface contact by setting the lower surface of the shoulder as the master surface, and the upper surface of the plate to be welded as the slave surface. The type of behaviour in contact is assumed tangential friction with generation of heat. Table 4 summarizes the contact properties used in this study. As given in the table, it has been assumed that all of the dissipated energy will be transformed into heat. Half of this heat will be transmitted and distributed over the surface of the HDPE plate.

Table 4. Plate/tool contact properties.

Friction coefficient	Heat generation	
0.3	Fraction of energy dissipated and transformed into heat (%)	Fraction of heat distributed to the slave surface (%)
	100	50

RESULTS AND DISCUSSION

Mechanical analysis

Results of pressure and equivalent stress distribution for different combinations of welding parameters are presented in this section.

Figures 5a and 5b show the pressure on the plates at the end of the plunging phase with a tool rotation speed of 2000 rpm and 500 rpm, respectively.

It is clear from Fig. 5 that a maximum pressure is located exactly under the shoulder at the tool/plate interface. In addition, it is noticed that negative pressure is produced far from the tool edge. In fact, this is right for high rotational speed as illustrated in Figs. 6a and 6b. These present the pressure distribution along the transverse line through the centre of the shoulder. Thereby, Figs. 6a and 6d show the pressure distribution across the surface of the two plates, along the line through the welded joint. These curves reveal the important effect of rotational speed on pressure distribution. It is clearly observed that for the same pressure exerted on the tool, the pressures generated in the plates are different for two different rotational speeds (Figs. 6a and 6b). This is the result obtained for the shoulder radius R = 10 mm. On the other hand, the curves in Figs. 6c and 6d reveal an equal pressure distribution whatever the speed of rotation, for the minimum shoulder radius R = 5 mm. Another fact noted for the small diameter is the non-existence of negative pressures (Figs. 6c and 6d).

Von Mises equivalent stress distributions are shown in Fig. 7. It can be seen that equivalent stresses are locally important. Higher values are noted for higher rotational speed (2000 rpm).

Consequently, plastic deformations may occur within the material of the plates which would imply additional heat releases due to the energy of the plastic deformations. The comparison between results illustrated in Figs. 7 highlights an important fact.

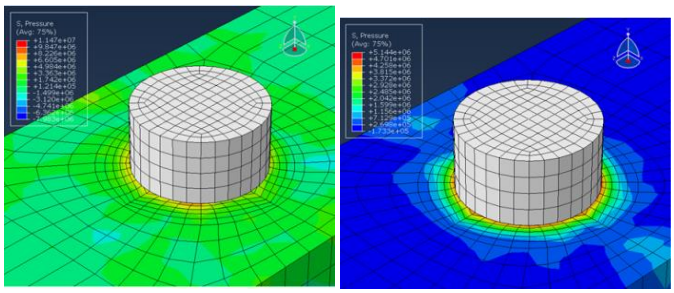

(a) (b)

Figure 5. The pressure state at the end of plunge phase for: a) rotation speed of 2000 rpm; and b) rotation speed of 500 rpm.

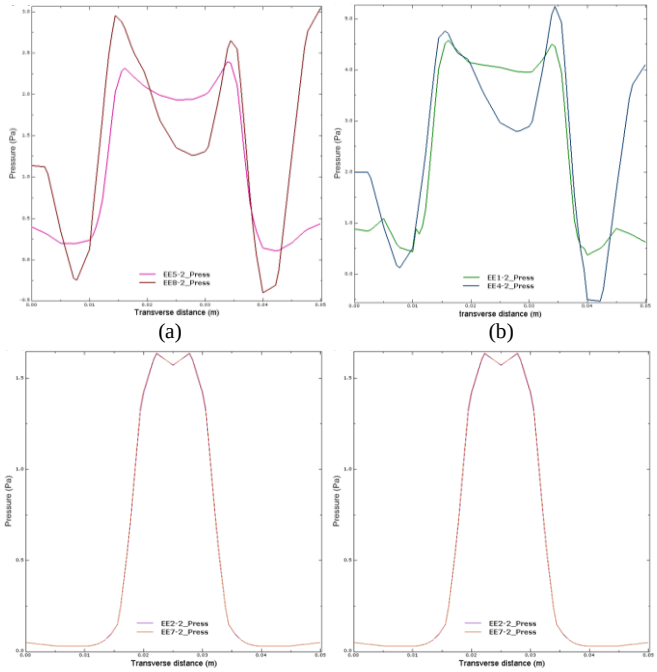

(a) (b)

(c) (d)

Figure 6. Pressure distribution along the transverse line, through the welded joint, at the end of the plunging phase for rotation speeds of: a) 2000 rpm; and b) 500 rpm.

EE	w (rpm)	D (mm)	P (MPa)
EE1_2:	500	20	10
EE2_2:	500	10	5
EE3_2:	2000	10	10
EE4_2:	2000	20	10
EE5_2:	500	20	5
EE6_2:	500	10	10
EE7_2:	2000	10	5
EE8_2:	2000	20	5

Indeed, it is observed that the same force exerted by the tool produces two different stress states in the plates to be welded by a tool of diameter 20 mm (Figs. 7a and 7b). This depends on rotational speed. Thus, a pressure of 10 MPa produces maximum stresses of 12 MPa with a rotation of 2000 rpm. However, this same pressure produces maximal stresses of 8 MPa with a rotation of 500 rpm (Fig. 7a).

On the other hand, a diameter of 10 mm creates a similar state of stress whatever the tool rotational speed. This is clearly illustrated in Figs. 7c and 7d. Therefore, this leads one to predict that the rotational speed amplifies the stresses in plates. That said, a rotation speed of 2000 rpm induces higher stresses than those induced by a rotation of 500 rpm.

Thermal analysis - heat flux

In order to estimate heat fluxes generated locally at the tool/plate interface, different iso-values obtained for different combinations of welding parameters are illustrated in Fig. 8. It is clear from this figure that the main source of heat flow is the tool. The latter, by friction of the shoulder with the surface of the plates, generates heat which flows through the interface of the plates.

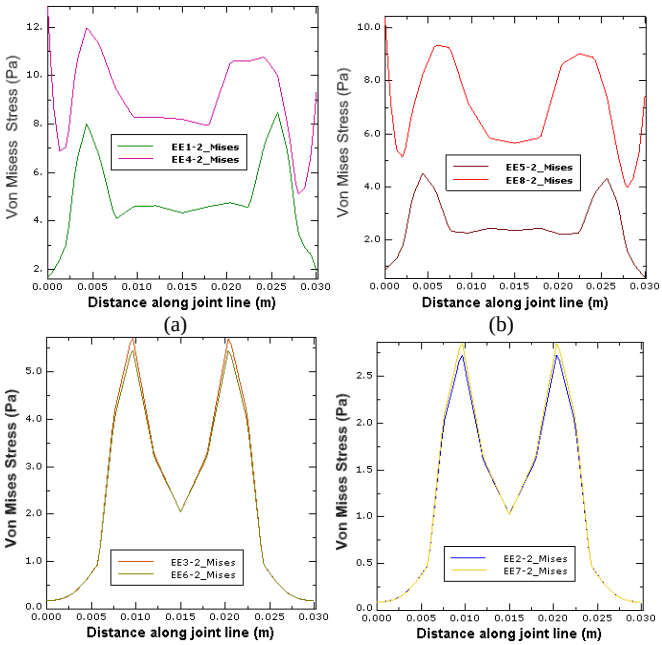

(a) (b)

(c) (d)

Figure 7. Comparison of rotational speed effect on Von Mises stresses along the joint.

EE	w (rpm)	D (mm)	P (MPa)
EE1_2:	500	20	10
EE2_2:	500	10	5
EE3_2:	2000	10	10
EE4_2:	2000	20	10
EE5_2:	500	20	5
EE6_2:	500	10	10
EE7_2:	2000	10	5
EE8_2:	2000	20	5

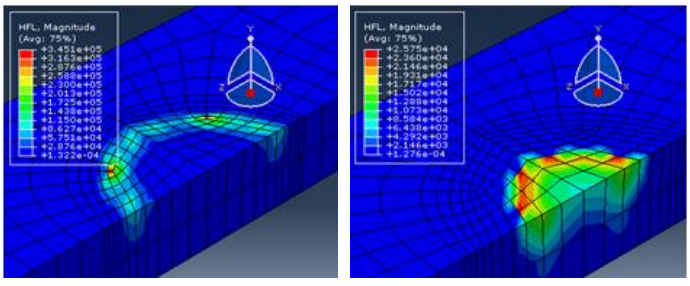

Figure 8. Heat flux generated in the plate.

Mainly, it can be seen that the small diameter concentrates heat fluxes in the vicinity of the welding joint, unlike large diameters that generate higher heat fluxes, but more dispersed and far from the welding joint. This implies that the heated area is wider and therefore a coarse welded joint is obtained. Consequently, it will be relevant to optimise the shoulder diameter while keeping a good compromise between rotational speed and pressure force.

The effect of diameter is clearly identified in Figs. 9a-d. First, one notices that rotational speed has a major influence on the produced heat flux. Figures 9a-b show distribution of heat fluxes generated by a maximal diameter (D = 20 mm), with maximal and minimal pressure 10 and 5 MPa, in respect. Both figures show a significant increase in flow by increasing rotational speed. It should be noted that the flow around the tool is not homogeneous. Thus, for a rotational speed of 2000 rpm, a peak flux difference of 2.105 W is noted. However, it can be predicted that the temperature will be distributed in a non-homogeneous manner, which will justify an additional hold time. On the other hand, a lower shoulder diameter (D = 10 mm) produces similarly distributed heat flow around the tool, Figs. 9c-d.

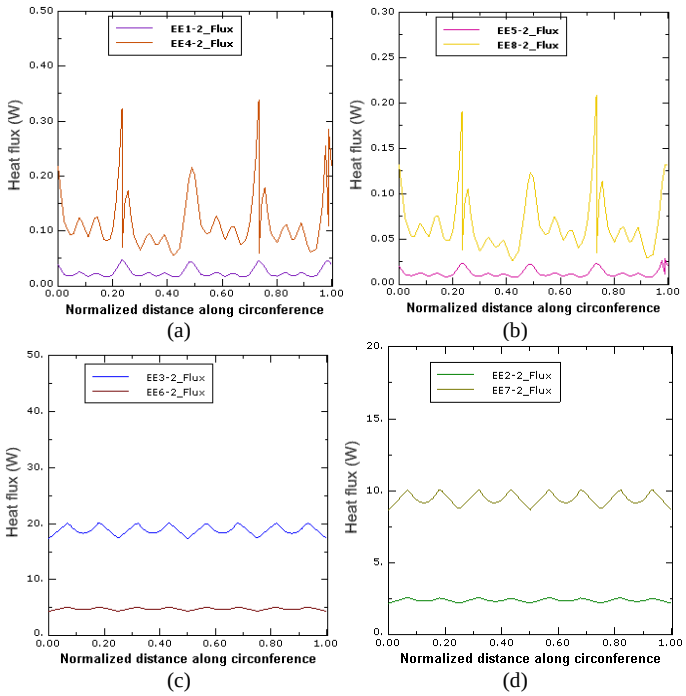

Figure 9. Effect of rotational speed on heat flow around shoulder.

EE	w (rpm)	D (mm)	P (MPa)
EE1_2:	500	20	10
EE2_2:	500	10	5
EE3_2:	2000	10	10
EE4_2:	2000	20	10
EE5_2:	500	20	5
EE6_2:	500	10	10
EE7_2:	2000	10	5
EE8_2:	2000	20	5

Temperature

To examine the performance of FSW parameters and, as consequence, the quality of the welded joint, it is important to have sufficient information on the reached temperature during the welding process. In fact, FSW welding is done in the solid state, where the temperature is kept below melting point while softening the material. For this purpose, the reference temperature is considered between 110 and 120°C for HDPE which melts at nearly 130 °C, /33/. Thus, for optimisation reasons, the target temperature is taken at T = 115 °C, which would make it possible to judge the efficiency of the welding parameters of FSW. Simulation results with various combinations of parameters are then analysed.

Figure 10 illustrates the temperature distribution over the work piece surface and around the shoulder. It is clear that temperatures much higher than the melting point of the material can be obtained. This would imply a local overflow of material and consequently a deterioration of the welded joint. Likewise, much lower temperatures can be obtained, but obviously prevents softening of the material and consequently difficult and even impossible.

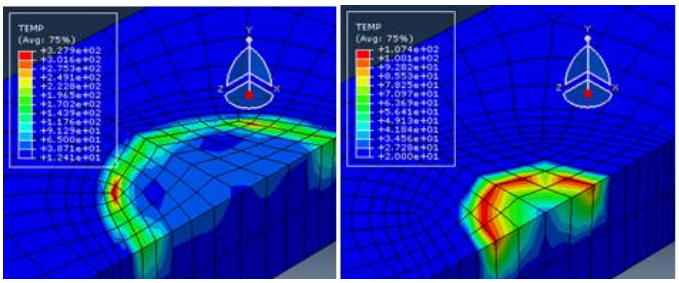

Figure 10. Temperature distributions over the workpiece surface.

In order to better distinguish effects of different welding parameters, it is judicious to compare temperature distributions around the circumference of the shoulder, because at this location the temperature peaks are raised.

Thus, to analyse the effect of tool speed, the temperature curves around shoulder are presented in Figs. 11a-d. Figure 11a shows comparison of temperatures obtained by two rotational speeds, 500 (EE1-2) and 2000 rpm (EE4-2). Pressure load and shoulder diameter are kept 10 MPa and 20 mm, in respect. Figure 11b presents the same comparison for 5 MPa and 10 mm. From these figures, the rotational speed affects significantly the temperature values. This effect is all the more marked for larger tool diameter (D = 20 mm, Figs. 11a-b). Indeed, a smaller tool diameter (D = 10 mm) produces relatively lower temperatures, especially when the rotation speed is minimal (w = 500 rpm, Figs. 11c-d).

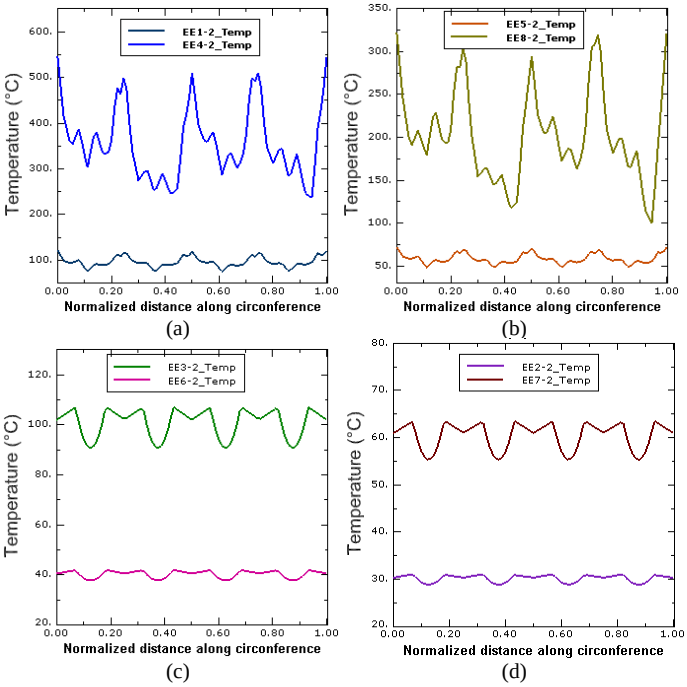

Figure 11. Comparison of rotational speed effects on temperatures generated at the plate/tool interface.

EE	w (rpm)	D (mm)	P (MPa)
EE1_2:	500	20	10
EE2_2:	500	10	5
EE3_2:	2000	10	10
EE4_2:	2000	20	10
EE5_2:	500	20	5
EE6_2:	500	10	10
EE7_2:	2000	10	5
EE8_2:	2000	20	5

In addition, the effect of pressure is shown in Figs. 12a-c. Figure 12a presents a comparison of temperatures obtained by two exerted pressures 5 (EE5-2) and 10 MPa (EE1-2). The other two parameters are identical and are w = 500 rpm and D = 20 mm for rotation speed and shoulder diameter. Likewise, Fig. 12b presents a comparison of temperatures obtained by two pressures 5 (EE8-2) and 10 MPa (EE4-2), and the other two parameters are the same, respectively, w = 2000 rpm and D = 20 mm. From these figures, it can be seen that pressure has a significant effect on temperature values reached under the tool shoulder, but with relatively less dispersion.

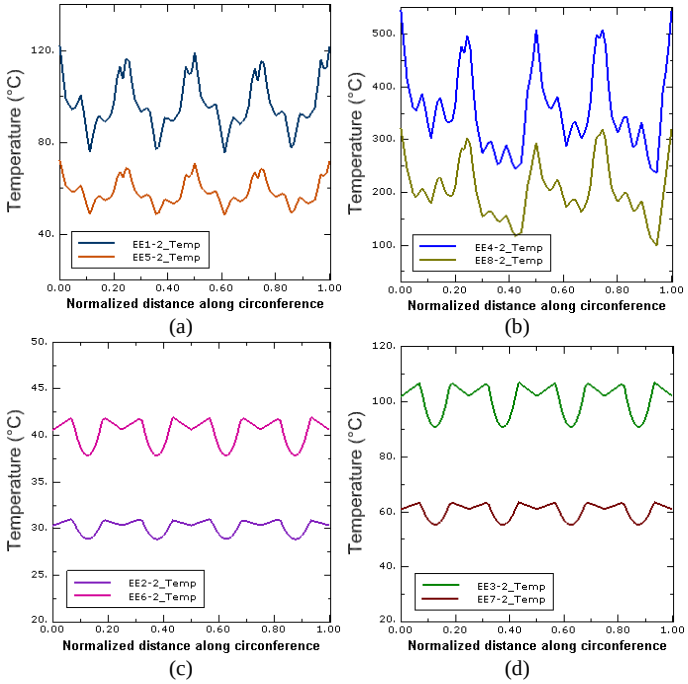

Figure 12. Effect of tool pressure on temperature distribution in the welded joint.

EE	w (rpm)	D (mm)	P (MPa)
EE1_2:	500	20	10
EE2_2:	500	10	5
EE3_2:	2000	10	10
EE4_2:	2000	20	10
EE5_2:	500	20	5
EE6_2:	500	10	10
EE7_2:	2000	10	5
EE8_2:	2000	20	5

MAIN EFFECTS OF WELDING PARAMETERS

Plots of the main effects of each parameter and their interactions on maximum temperature response for friction stir welding are shown in Figs. 13 and 14, in respect. As shown in Fig. 13, the temperature of the weld increases directly with tool rotational speed, load pressure, and tool shoulder diameter. Analysing the main effects plots, it is found that a target temperature of 115 °C is achieved using a combination of 1250 rpm rotational speed, 7.5 MPa load pressure, and 16.35 mm shoulder diameter (Fig. 13).

Figure 14 illustrates interaction effects. It is shown that tool rotational speed has an important role in the reached temperature during the welding process. Also, the shoulder diameter has an important effect in the temperature output. Thus, a right combination of parameters is crucial to achieve an efficient and qualitative welded joint. That said, large shoulder diameter combined with high tool rotational speed provides higher local temperature due to larger frictional area and short allocated time for material heating, /32/.

Figure 15 presents the iso-surfaces contour plots of temperature responses. Figures 15a-c present contours in quasi-linear sectors. Consequently, a relative strong dependence of parameter effects is stated, namely the rotational speed, shoulder diameter, and pressure exerted by the tool, at constant optimum values of 1250 rpm, 16.32 mm, and 7.5 MPa. Indeed, Fig. 15a shows that the target temperature is highly sensitive to the change in rotational speed. This is reflected by a high slope of the temperature surface bands. Figure 15b shows that the change in diameter of the shoulder is slightly less sensitive than the change in rotational speed. Exhibiting lower slopes, the temperature surfaces suggest a low sensitivity to changes in diameter and pressure as shown in Fig. 15c.

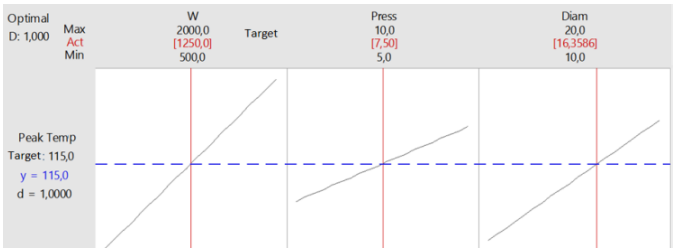

Figure 13. Plots of main effects of parameters on peak temperature.

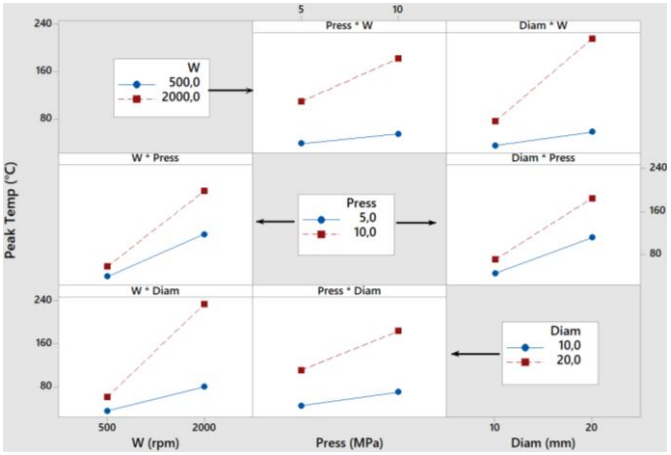

Figure 14. Plots of interacting effects of parameter combinations on peak temperature.

CONCLUSIONS

A 3-D finite element model of friction stir welding of polyethylene plate is performed. The effects of tool rotational speed, tool diameter and tool pressure on mechanical and thermal responses are analysed and optimised.

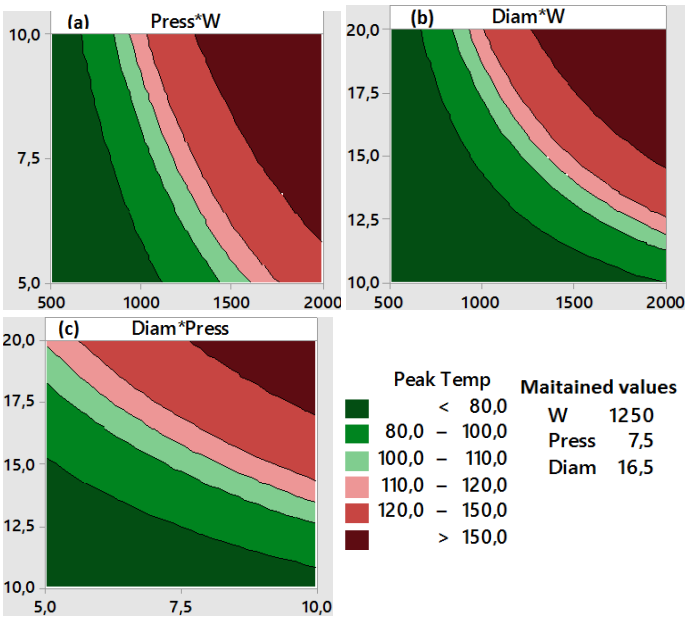

Figure 15. Iso-surfaces plots of peak temperature.

The main conclusions are as follows:

– Same pressure produces different stress states in the plates when using high shoulder diameter and varying rotational speed. However, lower shoulder diameter creates a similar state of stress whatever the tool rotational speed.
– Heat flux is more concentrated in the vicinity of the welded joint when using lower shoulder diameter. Larger diameter generates higher heat fluxes, but more dispersed and far from the welded joint. Consequently, the heated area is wider and therefore, a coarse welded joint may be obtained.
– Temperatures well above melting point of material are obtained if the combination of welding parameters is incorrectly chosen. i.e. if high speed is combined with an inadequate diameter, producing excessive pressure.
– On the contrary, temperatures well below the softening point of the material can be obtained. This depends on the correct choice of welding parameters.
– Desirable temperature of 115 °C can be achieved using a combination of 1250 rpm rotational speed, 7.5 MPa load pressure, and 16.35 mm shoulder diameter.
– The tool rotational speed has the most important role in the temperature response during the welding process. In second order, the shoulder diameter has significant effect in the temperature localization. Pressure exerted by the tool has the lower effect on the temperature.

REFERENCES

1. Freeman, R., Friction Stir Welding (FSW), TWI Bulletin, 2003, The Welding Institute (TWI).
2. Mehta, K.P., Badheka, V.J. (2016), *A review on dissimilar friction stir welding of copper to aluminum: process, properties, and variants*, Mater. Manufac. Proc. 31(3): 233-254. doi: 10.1080/10426914.2015.1025971
3. Murr, L.E. (2010), *A review of FSW research on dissimilar metal and alloy systems*, J Mater. Eng. Perform. 19: 1071-1089. doi: 10.1007/s11665-010-9598-0
4. Zahaf, S., Zina, S., Bouaziz, B., et al. (2019), *Optimisation of FSW welding parameters on maximal temperature, Von Mises and residual stresses, and equivalent plastic deformation applied to a 6061 aluminium alloy*, Struct. Integ. and Life, 19(3): 195-209.
5. Saleh, A.A. (2020), *Joining of AA2014 and AA5059 dissimilar aluminium alloys by friction stir welding*, Struct. Integ. and Life, 20(2): 99-102.
6. Habib, L., Azzeddine, H., Lahouari, B. (2020), *Experimental study of tensile shear test in friction stir spot welding*, Struct. Integ. and Life, 20(2): 173-175.
7. Živković, A., Đurđević, A., Sedmak, A., et al. (2015), *Friction stir welding of aluminium alloys - T joints*, Struct. Integ. and Life, 15(3): 181-186.
8. Đurđević, A., Tadić, S., Ivanović, I., et al. (2017), *Numerical analysis of heat transfer during friction stir welding*, Struct. Integ. and Life, 17(1): 45-48.
9. Ivanović, I., Sedmak, A., Miloš, M., et al. (2011), *Numerical study of transient three-dimensional heat conduction problem with a moving heat source*, Thermal Sci. 15(1): 257-266. doi: 10.2298/TSCI1101257I
10. Veljić, D., Perović, M., Sedmak, A., et al. (2011), *Numerical simulation of the plunge stage in friction stir welding*, Struct. Integ. and Life, 11(2): 131-134.
11. Veljić, D., Perović, M., Sedmak, A., et al. (2012), *A coupled thermo-mechanical model of friction stir welding*, Thermal Sci. 16(2): 527-534.
12. Murariu, A.C., Veljić, D., Barjaktarević, D., et al. (2016), *Influence of material velocity on heat generation during linear welding stage of friction stir welding*, Thermal Sci. 20(5): 1693-1701. doi: 10.2298/TSCI150904217M
13. Veljić, D., Sedmak, A., Rakin, M., et al. (2014), *Experimental and numerical thermo-mechanical analysis of friction stir welding of high-strength aluminium alloy*, Thermal Sci. 18(Suppl. 1): S29-S38. doi: 10.2298/TSCI130512171V
14. Schmidt, H., Hattel, J., Wert, J. (2003), *An analytical model for the heat generation in friction stir welding*, Model. Simul. Mater. Sci. Eng. 12(1): 143-157. doi: 10.1088/0965-0393/12/1/013
15. Gadakh, V.S., Adepu, K. (2013), *Heat generation model for taper cylindrical pin profile in FSW*, J Mater. Res. Technol. 2 (4): 370-375. doi: 10.1016/j.jmrt.2013.10.003
16. Kumar, R., Singh, R., Ahuja, I.P.S., et al. (2018), *Weldability of thermoplastic materials for friction stir welding- A state of art review and future applications*, Compos. Part B: Eng. 137: 1-15. doi: 10.1016/j.compositesb.2017.10.039
17. Singh, S., Prakash, C., Gupta, M.K. (2020), *On friction-stir welding of 3D printed thermoplastics*, In: Materials Forming, Machining and Post Processing, Springer, Cham, pp.75-91. doi: 10.1007/978-3-030-18854-2_3
18. Derazkola, H.A., Eyvazian, A., Simchi, A. (2020), *Modeling and experimental validation of material flow during FSW of polycarbonate*, Mater. Today Comm. 22: 100796. doi: 10.1016/j.mtcomm.2019.100796
19. Mendes, N., Neto, P., Simão, M.A., et al. (2016), *A novel friction stir welding robotic platform: welding polymeric materials*, Int. J Adv. Manuf. Technol. 85: 37-46. doi: 10.1007/s00170-014-6024-z
20. Lambiase, F., Derazkola, H.A., Simchi, A. (2020), *Friction stir welding and friction spot stir welding processes of polymers - State of the art*, Materials (Basel), 13(10): 2291. doi: 10.3390/ma13102291
21. Mishra, D., Roy, R.B., Dutta, S., et al. (2018), *A review on sensor based monitoring and control of friction stir welding process and a roadmap to Industry 4.0*, J Manufac. Proc. 36: 373-397. doi: 10.1016/j.jmapro.2018.10.016

22. Schmidt, H., Hattel, J. (2005), *Modelling heat flow around tool probe in friction stir welding*, Sci. Technol. Weld. Join. 10(2): 176-186. doi: 10.1179/174329305X36070
23. Zimmer, S., Langlois, L., Laye, J., Bigot, R. (2010), *Experimental investigation of the influence of the FSW plunge processing parameters on the maximum generated force and torque*, Int. J Adv. Manuf. Technol. 47: 201-215. doi: 10.1007/s00170-009-2188-3
24. Nallusamy, S. (2015), *Analysis of welding properties in FSW aluminium 6351 alloy plates added with silicon carbide particles*, Int. J Eng. Re. Africa, 21: 110-117. doi: 10.4028/www.scientific.net/JERA.21.110
25. Eslami, S., de Figueiredo, M.A.V., Tavares, P.J., Moreira, P.M. G.P. (2018), *Parameter optimisation of friction stir welded dissimilar polymers joints*. Int. J Adv. Manuf. Technol. 94: 1759-1770. doi: 10.1007/s00170-017-0043-5
26. Huang, Y., Meng, X., Xie, Y., et al. (2018), *Friction stir welding/processing of polymers and polymer matrix composites*, Compos. Part A: Appl. Sci. Manufac. 105: 235-257. doi: 10.1016/j.compositesa.2017.12.005
27. Elyasi, M., Derazkola, H.A. (2018), *Experimental and thermo-mechanical study on FSW of PMMA polymer T-joint*, Int. J Adv. Manuf. Technol. 97(1-4): 1445-1456. doi: 10.1007/s00170-018-1847-7
28. Selvamani, S.T., Vigneshwar, M., Divagar, S. (2015), *Effects of heat transfer on microhardness and microstructure of friction stir welded AA 6061 aluminum alloy*, Int. J Eng. Res. Africa, 21: 102-109. doi: 10.4028/www.scientific.net/JERA.21.102
29. Abdallah, L., El Bahri, O.C., Miloud, M.H., (2018), *Parametric study of the mechanical behavior of FSSW welded polymer plates using a new form of welding tool*, Defect Diffus. Forum, 389: 205-215. doi: 10.4028/www.scientific.net/DDF.389.205
30. kaddour, H., Hadj Miloud, M., El Bahri, O.C., et al. (2019), *Mechanical behavior analysis of a Friction Stir Welding (FSW) for welded joint applied to polymer materials*, Frattura ed Integrità Strutturale, 13(47): 459-467. doi: 10.3221/IGF-ESIS.47.36
31. Dascau, H., Kirin, S., Sedmak, A., et al. (2015), *Crack resistance of aluminium alloy friction stir welded joint*, Struct. Integ. and Life, 15(1): 51-54.
32. Veljić, D., Sedmak, A., Rakin, M., et al. (2015), *Advantages of friction stir welding over arc welding with respect to health and environmental protection and work safety*, Struct. Integ. and Life, 15(2): 111-116.
33. Eslami, S., Miranda, J.F., Mourão, L., et al. (2018), *Polyethylene friction stir welding parameter optimization and temperature characterization*, Int. J Adv. Manufac. Technol. 99(1): 127-136. doi: 10.1007/s00170-018-2504-x
34. Raouache, E., Boumerzoug, Z., Rajakumar, S., Khalfallah, F. (2018), *Effect of FSW process parameters on strength and peak temperature for joining high-density polyethylene (HDPE) sheets*, Revue des Composites et des Matériaux Avancés, 28(2): 149-160. doi: 10.3166/RCMA.28.149-160

ESIS ACTIVITIES

CALENDAR OF CONFERENCES, TC MEETINGS, and WORKSHOPS

September 12-14, 2022	TC2 meeting – Tenth International Conference on MATERIALS STRUCTURE & MICROMECHANICS OF FRACTURE (MSMF10)	ESIS - TC2, Brno, Czech Republic	https://msmf.fme.vutbr.cz/
June 25–26, 2022	7th Summer School on 'Fracture Mechanics and Structural Integrity'	Funchal, Madeira, Portugal	link
June 27–July 01, 2022	23rd European Conference on Fracture - ECF23	Funchal, Madeira, Portugal	link